

PACS numbers: 42.55.Rz; 42.55.Ks; 42.60.Jf; 42.60.Lh
DOI: 10.1070/QE2015v045n09ABEH015845

Scaling of energy characteristics of polycrystalline Fe^{2+}:ZnSe laser at room temperature

E.M. Gavrishchuk, V.B. Ikonnikov, S.Yu. Kazantsev, I.G. Kononov,
S.A. Rodin, D.V. Savin, N.A. Timofeeva, K.N. Firsov

Abstract. **The lasing characteristics of lasers based on diffusion-doped Fe^{2+}:ZnSe polycrystalline samples excited at room temperature by an electric-discharge HF laser are studied. A sample doped from two sides (working surfaces) emitted laser radiation with the energy $E = 253$ mJ with the slope efficiency $\eta_d = 33\%$ and the efficiency with respect to the absorbed energy $\eta_{abs} \approx 28\%$ in the case of an elliptical pump spot of size $a \times b = 6.8 \times 7.5$ mm. It is found that the possibility of increasing the lasing energy of the samples of these types by increasing the pump spot area (at a constant pump energy density) is limited by the appearance of parasitic generation typical for disk lasers. The first results are reported on the laser based on a polycrystalline sample made by a technology that allows one to form a zero dopant concentration on the surface and a maximum concentration inside the sample (i.e., to create a sample with internal doping). The possibilities of increasing the Fe^{2+}:ZnSe laser energy at room temperature by using multilayer samples fabricated by this doping method are discussed.**

Keywords: *Fe^{2+}:ZnSe laser, non-chain electric-discharge HF laser, optical pumping, diffusion doping, CVD method, barothermic treatment.*

1. Introduction

Optically pumped Fe^{2+}:ZnSe lasers attract attention of researches by the possibility of obtaining high-power coherent radiation in the practically important spectral range 4–5 μm [1–16]. To date, the maximum energy ($E = 4.9$ J) of a Fe^{2+}:ZnSe laser with the efficiency with respect to the absorbed energy $\eta_{abs} \approx 47\%$ was obtained by the authors of [14] under pumping by a free-running Er:YAG laser at a temperature $T = 85$ K. For practical applications, it is preferable to use lasers operating at room temperature. However, as was shown in [14], an increase in temperature to room temperature in the case of a free-running pump laser led to a decrease in E to 53 mJ ($\eta_{abs} < 1\%$) due to decreasing lifetime of the upper laser state $^5T_2$ of Fe^{2+} ions in the ZnSe matrix (~360 ns at room temperature [8]). Under pumping by a short solid-state laser pulse (Q-switching mode), the maximum energy E and slope efficiency η_d at room temperature were 6 mJ and 39%, respectively [15], and the possibility of a further increase in the energy was limited by the low energy characteristics (maximum energy 35 mJ [6]) of available three-micron solid-state Q-switched lasers used for pumping the Fe^{2+}:ZnSe crystal.

The energy of room-temperature Fe^{2+}:ZnSe lasers has been considerably increased by using non-chain electric-discharge HF lasers as pump sources [10–14]. Their spectrum ($\lambda = 2.6–3.1$ μm) completely falls into the absorption band of Fe^{2+} in ZnSe crystal. These lasers emit short (100–200 ns) light pulses and almost unlimited energy from the viewpoint of applications considered in this work (see [17–19] and references therein). It is also important that these lasers can operate with high pulse repetition rates [20, 21]. The maximum output pulse energy E of a Fe^{2+}:ZnSe polycrystal diffusion-doped through both faces in the case of pumping by a HF laser at room temperature was 192 mJ with $\eta_{abs} = 23\%$ [12]. In the repetitively pulsed regime, the average power of a Fe^{2+}:ZnSe laser pumped by a HF laser [13, 14] was 2.4 W with a pulse energy up to 14 mJ [14] (pulse repetition rate up to 200 Hz).

The aim of the present work is to study the possibility of increasing the output energy of lasers based on Fe^{2+}:ZnSe polycrystalline samples pumped by a pulsed electric-discharge HF laser at room temperature.

2. Experimental setup

In experiments, we used two types of active polycrystalline Fe^{2+}:ZnSe elements. The samples of the first type were made of polycrystalline ZnSe grown by chemical vapour deposition (CVD) in the reaction of zinc vapour and hydrogen selenide in an Ar flow. From this material, we cut plates 20 mm in diameter and 4.5 mm thick, which were then mechanically ground and polished. The method of doping ZnSe crystals with Fe ions did not considerably differ from the method of doping with Cr ions [22]. Both surfaces of the ZnSe plate were coated with Fe films no thicker than 1 μm by electron-beam deposition. The plates were annealed for 7–15 days at a tem-

E.M. Gavrishchuk G.G. Devyatykh Institute of Chemistry of High-Purity Substances, Russian Academy of Sciences, ul. Tropinina 49, 603950 Nizhnii Novgorod, Russia; N.I. Lobachevskii Nizhnii Novgorod State University, ul. Gagarina 23, 603950 Nizhnii Novgorod, Russia; e-mail; gavr@ihps.nnov.ru;
V.B. Ikonnikov, S.A. Rodin, D.V. Savin, N.A. Timofeeva G.G. Devyatykh Institute of Chemistry of High-Purity Substances, Russian Academy of Sciences, ul. Tropinina 49, 603950 Nizhnii Novgorod, Russia; e-mail: ikonnikov@ihps.nnov.ru, rodin@ihps.nnov.ru;
S.Yu. Kazantsev, I.G. Kononov A.M. Prokhorov General Physics Institute, Russian Academy of Sciences, ul. Vavilova 38, 119991 Moscow, Russia; e-mail: kazan@kapella.gpi.ru, kononov@kapella.gpi.ru;
K.N. Firsov A.M. Prokhorov General Physics Institute, Russian Academy of Sciences, ul. Vavilova 38, 119991 Moscow, Russia; National Research Nuclear University 'MEPhI', Kashirskoe sh. 31, 115409 Moscow, Russia; e-mail: k_firsov@rambler.ru

Received 27 April 2015; revision received 10 June 2015
Kvantovaya Elektronika **45** (9) 823–827 (2015)
Translated by M.N. Basieva

perature of 1000±2°C in a sealed quartz tube filled with hydrogen. The annealed samples were chemically and mechanically polished. Sample No. 1 was annealed for 15 days, and sample No. 2 was annealed for 7 days. Sample 2 was used by us previously as an active element in [11–13].

The active element of the second type (sample No. 3) was prepared by an original technology described in detail in [23, 24] for Cr^{2+}:ZnSe crystals. An advantage of this technology is that it allows one to fabricate samples with a zero dopant concentration at the surface and a maximum concentration inside the sample (we call it the sample with internal doping). The process of fabrication of Fe^{2+}:ZnSe samples with internal doping has some specific features, which make it possible to produce a material of a higher optical quality with a precisely specified number of iron ions in the absorbing layer per unit area. First, the Fe^{2+}:ZnSe samples 10×15×5 mm in size obtained by the CVD method were coated by an iron film by the CVD method using the reaction of Zn vapours with $FeCl_2$. Then, to form a near-surface layer doped with Fe^{2+} ions, the samples were annealed in sealed quartz tubes at a temperature of 1050 °C in an argon atmosphere at a pressure of ~1 atm for two days. The optical absorption of iron ions in the samples (the number of iron ions in the absorbing layer per unit area) was controlled by Fourier transform IR spectroscopy.

Next, the samples were chemically and mechanically polished by the method described in [25] and placed into a CVD reactor to grow a ZnSe layer with a needed thickness on the surface doped with Fe^{2+} ions. As a result, we obtained a three-layer structure ZnSe–Fe^{2+}:ZnSe–ZnSe with a thickness up to 8 mm. To create a required iron concentration profile, we performed high-temperature gas-static treatment of the synthesised structure in an argon atmosphere at a pressure of 90 MPa and a temperature of 1200 °C for 53 h. The use of a high isostatic pressure considerably decreases the sublimation of zinc selenide and allows one to increase the temperature and decrease the time of the treatment compared to diffusion annealing. In addition, barothermal processing leads to healing of light-scattering bulk structural defects [26]. The size of sample 3 was 10×15×7 mm, and its lateral faces were roughly ground.

All the three samples had a similar transmission (3%–4%) at the pump wavelengths at low incident energy densities, and the surface density of ions in the absorbing layer (or in two layers in the case of samples with two-side doping) was about $(3–4)\times10^{18}$ cm^{-2}.

The experimental scheme is shown in Fig. 1. The Fe^{2+}:ZnSe laser cavity 120 mm long was formed by a concave mirror M1 (gold coating on a quartz substrate) with the curvature radius R = 1 or 0.5 m and a plane output mirror M2. The output mirrors (interference coating on CaF_2 substrates) had the reflection coefficients ρ = 40% and 60% at the wavelength λ = 4.5 μm. The Fe^{2+}:ZnSe samples were placed perpendicular to the optical axis of the cavity at a distance of 40 mm from the output mirror. The radiation of a high-power pulsed HF laser with the pulse full width at half maximum $\tau \approx$ 130–160 ns (depending on the concentration ratio of components in the working mixture) [10–12, 27, 28] was attenuated by calibrated optical filters F and focused on the sample surface by a spherical lens L with a focal distance of 45 cm into an elliptical spot with axes a and b. In the process of experiments, the pump spot area S containing 0.9 of the energy incident on the sample surface varied from 0.057 to 0.48 cm^2 (the major axis b of the pump spot ellipse was changed within 2.6–8.1 mm, while the b/a ratio varied from 1.02 to 1.08). The angle of incidence of the pump beam on the sample surface was ~20°. The pump radiation energy incident on the sample, the energy passed through the sample, and the Fe^{2+}:ZnSe laser output energy were measured by calorimeters C1–C3 (Molectron), respectively. To control the shape of pulses of the Fe^{2+}:ZnSe and HF lasers, we used photodetectors (Vigosystem Ltd) with a time resolution of ~1 ns. The high sensitivity of photodetectors allowed us to measure the radiation scattered from the receiving plates of corresponding calorimeters.

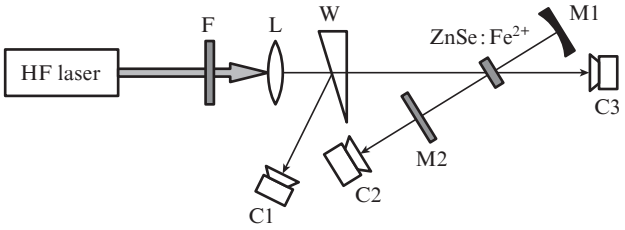

Figure 1. Experimental scheme: (W) BaF_2 wedge; (C1 – C3) calorimeters; (F) optical filters; (L) spherical lens; (Fe^{2+}:ZnSe) active element; (M1, M2) cavity mirrors.

When measuring the dependences of transmission of samples on the incident pump energy in the absence of Fe^{2+}:ZnSe laser oscillation, the cavity mirrors were shielded by non-reflective screens.

3. Experimental results and discussion

Figure 2 presents the dependences of transmission T of sample 1 on the incident HF laser energy density W_{in} measured in the absence of Fe^{2+}:ZnSe lasing at different dimensions a and b of the pump spot on the sample surface. One can see that the transmission behaviour strongly depends on the spot size. At relatively small spots ($b \leqslant 5.4$ mm), the transmission monotonically increases with increasing pump energy density W_{in} with a slight tendency to saturation. At $6.6 < b \leqslant 7$ mm, the transmission is observed to saturate at $W_{in} \approx 0.7$ J cm^{-2}. An increase in b to 8.1 mm leads to saturation already at $W_{in} \approx 0.4$ J cm^{-2}. This behaviour of the

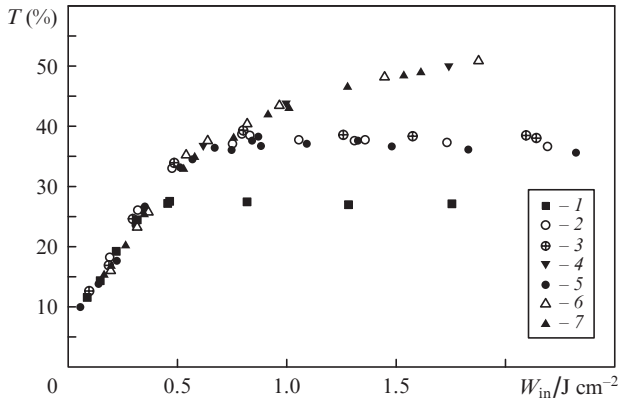

Figure 2. Dependences of the transmission T of sample 1 on the incident HF-laser energy density W_{in} in the absence of lasing at the pump spot sizes $a\times b$ = (*1*) 7.6×8.1, (*2*) 6.6×7, (*3*) 6.3×6.8, (*4*) 5.3×5.4, (*5*) 6.3×6.6, (*6*) 4×4.1 and (*7*) 2.6×2.8 mm.

dependence of T on W_{in} clearly points to the development of parasitic generation (superluminescence) [27] at large pump spots in the near-surface layer of the sample, where the dopant concentration is highest and, hence, the active medium gain is maximum.

At open mirrors M1 and M2, lasing along the optical axis of the cavity is developed more rapidly that the parasitic generation in the near-surface layer of the sample until the major axis b of the pump spot reaches some critical value. This is illustrated by the dependences of the output energy density of the Fe^{2+}:ZnSe laser $W_{out} = E/S$ (S is the pump spot area) on W_{in} at different pump spot sizes (Fig. 3). It is seen that the points measured at different pump spot sizes well fall on one and the same curve. At $W_{in} > 0.25$ J cm^{-2}, the dependence $W_{out}(W_{in})$ is linear, which testifies to low radiative energy loss in the direction transverse to the optical axis despite the large maximum size of the spot ($b = 7.8$ mm) in this series of experiments.

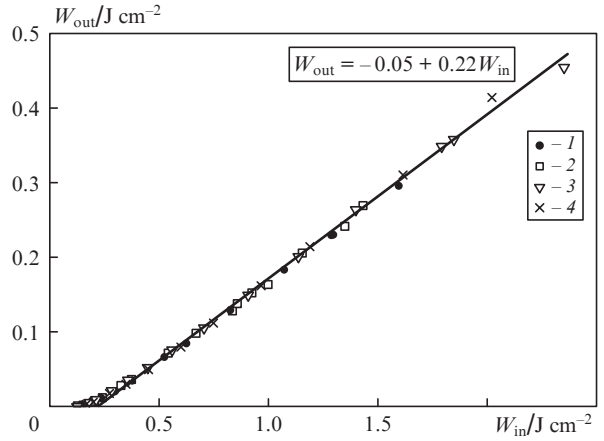

Figure 3. Dependences of the Fe^{2+}:ZnSe laser density W_{out} on the pump energy density W_{in} (sample 1) at the pump spot sizes $a \times b$ = (*1*) 4.5×4.7, (*2*) 5.3×5.4, (*3*) 6.8×7.1 and (*4*) 7.1×7.8 mm. The cavity parameters are $R = 1$ m and $\rho = 40\%$.

At large spots, it is also important to optimise the cavity parameters. Figure 4 shows the dependences of the Fe^{2+}:ZnSe laser energy on the energy E_{abs} absorbed in sample 2 at different combinations of ρ and R of cavity mirrors. The pump spot size ($a \times b = 6.8 \times 7.5$ mm) was the same as in [12]. One sees that the cavity optimisation makes it possible to noticeably increase the laser energy. At the M1 mirror curvature radius $R = 0.5$ m and the reflection coefficient of output mirror M2 $\rho = 40\%$, all the points on the plot (except for the point measured at the maximum E_{abs}) are well described by a linear function, the slope efficiency at the linear part being $\eta_d = 33\%$. The laser energy E reaches 253 mJ at $\eta_{abs} \approx 28\%$.

Thus, the optimisation of the cavity allowed us to increase the laser energy with respect to the energy obtained in [12] ($E = 192$ mJ) at the same spot size. However, already at $b > 8$ mm (similar to [12]) the laser energy decreased due to radiative losses in the direction transverse to the optical axis. Therefore, at the maximum pump energy density determined by the surface breakdown threshold (~3 J cm^{-2} [11]), the energy $E \approx 250$ mJ can obviously be considered as limiting for the Fe^{2+}:ZnSe disk laser elements diffusion-doped from two sides [29] (the maximum dopant concentration is achieved at the sample surface). Two-end pumping proposed in [11] will

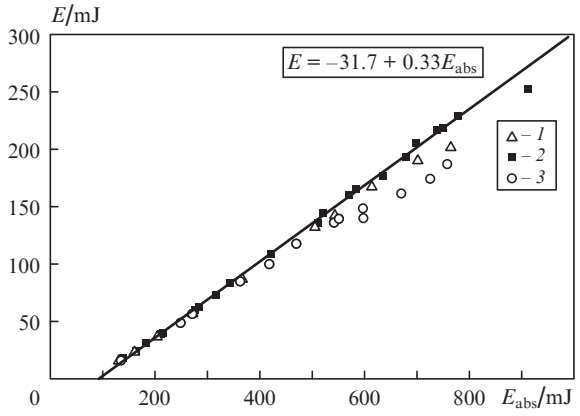

Figure 4. Dependences of the Fe^{2+}:ZnSe laser energy E on the HF laser energy E_{abs} absorbed in sample 2 at the cavity parameters (*1*) $\rho = 40\%$, $R = 1$ m; (*2*) 40%, 0.5 m; and (*3*) 60%, 1 m ($a \times b = 6.8 \times 7.5$ mm).

undoubtedly increase the laser energy, but this is not very convenient technically.

To further increase the energy of lasers based on Fe^{2+}:ZnSe polycrystal, it seems promising to create samples with several doped layers using the internal doping method proposed by the authors of [23, 24]. Such a multilayer sample, in which the Fe^{2+}:ZnSe layers are alternated with ZnSe layers, is schematically shown in Fig. 5. The maximum Fe^{2+} concentration in each of the doped layers must decrease inversely proportionally to the number of layers so that the multilayer sample transmission remained constant (close to the transmission of samples with two-side doping). Figure 6 presents the output energy of a Fe^{2+}:ZnSe laser based on sample 3, which is prepared by internal doping, as a function of the absorbed energy. The pump spot size was $a \times b = 4.7 \times 5$ mm. At $b > 5$ mm, the laser energy sharply decreased due to the development of parasitic generation caused, probably, by backscattering from the ground lateral surfaces of the crystal, i.e., the restriction by the spot size in this case is related to improper treatment of the crystal. As follows from Fig. 6, the slope efficiency of a laser based on a sample with internal doping is $\eta_d = 32\%$, and the efficiency with respect to the absorbed energy is $\eta_{abs} \approx 30\%$ at the maximum laser energy $E = 91$ mJ. Note that the lasing threshold for the sample with internal doping with respect to the absorbed energy ($E_{th} = 0.12$ J cm^{-2}) is almost twice as low as the lasing threshold for sample 1 with two-side doping ($E_{th} \approx 0.23$ J cm^{-2}), whose laser

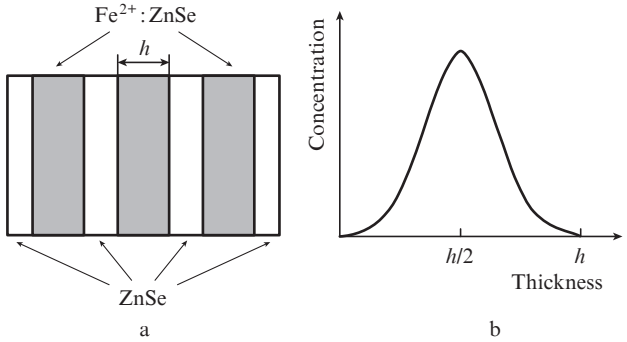

Figure 5. (a) Schematic of a multilayer sample prepared by the internal doping method and (b) Fe^{2+} concentration distribution in a doped layer with a thickness h.

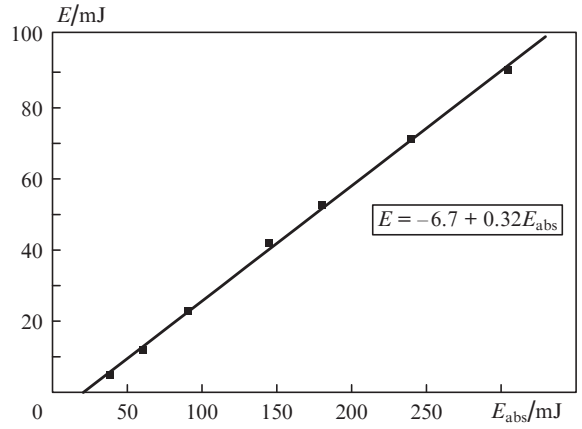

Figure 6. Dependence of the Fe^{2+}:ZnSe laser energy E on the absorbed HF laser energy E_{abs} for sample 3 prepared by internal doping ($a \times b$ = 4.7×5 mm, ρ = 60%, R = 1 m).

characteristics are shown in Fig. 4. Figure 7 presents the oscillograms of HF and Fe^{2+}:ZnSe laser pulses in the case of sample 3 at the absorbed energy E_{abs} = 250 mJ. Under this pumping, the Fe^{2+}:ZnSe laser pulse duration at half maximum is ~145 ns.

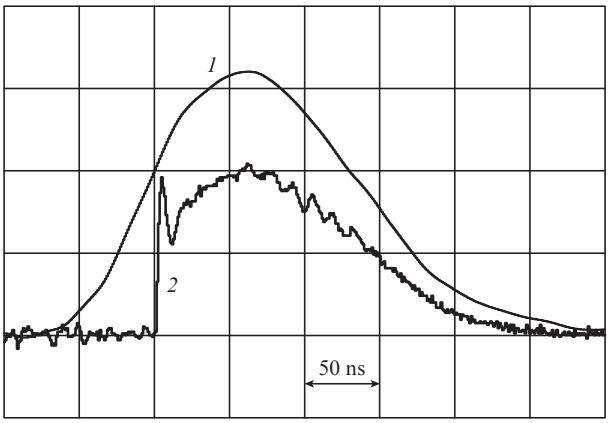

Figure 7. Oscillograms of (*1*) HF and (*2*) Fe^{2+}:ZnSe laser pulses; E_{abs} = 250 mJ.

Thus, the sample with internal doping is highly competitive in main characteristics with the samples doped from two sides. Therefore, we can expect that the development of the fabrication technology of polycrystalline Fe^{2+}:ZnSe samples with multilayer doping will make it possible to increase the laser energy by increasing the pump spot area.

4. Conclusions

We have studied the lasing characteristics of lasers based on polycrystalline diffusion-doped Fe^{2+}:ZnSe samples excited at room temperature by a pulsed non-chain HF laser. The energy of a sample doped through two faces was E = 253 mJ. It is established that a further increase in the laser energy of the samples of this type by increasing the pump spot area is limited by the development of parasitic generation typical for disk lasers. The possibilities of creating a high-energy laser based on multilayer samples fabricated by the internal doing method, in which the iron-doped ZnSe layers alternate with undoped layers, are discussed.

Acknowledgements. This work was supported by the Russian Scientific Foundation (Grant No. 15-13-10028) in the part concerning the development of technology and fabrication of ZnSe:Fe^{2+} samples and by the Russian Foundation for Basic Research (Grants Nos 15-08-02562 and 15-02-06005) in what concerns the development of experimental methods and carrying out the experiments.

References

1. Adams J.J., Bibeau C., Page R.H., Krol D.M., Furu L.H., Payne S.A. *Opt. Lett.*, **24** (23), 1720 (1999).
2. Kernal J., Fedorov V.V., Gallian A., Mirov S.B., Badikov V.V. *Opt. Express*, **13** (26), 10608 (2005).
3. Akimov V.A., Voronov A.A., Kozlovskii V.I., Korostelin Yu.V., Landman A.I., Podmar'kov Yu.P., Frolov M.P. *Kvantovaya Elektron.*, **36** (4), 299 (2006) [*Quantum Electron.*, **36** (4), 299 (2006)].
4. Il'ichev N.N., Danilov V.P., Kalinushkin V.P., Studenikin M.I., Shapkin P.V., Nasibov A.S. *Kvantovaya Elektron.*, **38** (2), 95 (2008) [*Quantum Electron.*, **38** (2), 95 (2008)].
5. Doroshenko M.E., Jelinkova H., Koranda P., Sulc J., Basiev T.T., Osiko V.V., Komar V.K., Gerasimenko A.S., Puzikov V.M., Badikov V.V., Badikov D.V. *Laser Phys. Lett.*, **7** (1), 39 (2010).
6. Myoung NoSoung, Martyshkin D.V., Fedorov V.V., Mirov S.B. *Opt. Lett.*, **36** (1), 94 (2011).
7. Doroshenko M.E., Jelinkova H., Sulc J., Jelinek M., Nemec M., Basiev T.T., Zagoruiko Y.A., Kovalenko N.O., Gerasimenko A.S., Puzikov V.M. *Laser Phys. Lett.*, **9** (4), 301 (2012).
8. Frolov M.P., Korostelin Yu.V., Kozlovsky V.I., Mislavskii V.V., Podmar'kov Yu.P., Savinova S.A., Skasyrsky Ya.K. *Laser Phys. Lett.*, **10**, 125001 (2013).
9. Mirov S.B., Fedorov V.V., Martyshkin D.V., Moskalev I.S., Mirov M.S., Vasilyev S.V. *IEEE J. Sel. Top. Quantum Electron.*, **21** (1), 1601719 (2015).
10. Velikanov S.D., Danilov V.P., Zakharov N.G., Il'ichev N.N., Kazantsev S.Yu., Kalinushkin V.P., Kononov I.G., Nasibov A.S., Studenikin M.I., Pashinin P.P., Firsov K.N., Shapkin P.V., Shchurov V.V. *Kvantovaya Elektron.*, **44** (2), 141 (2014) [*Quantum Electron.*, **44** (2), 141 (2014)].
11. Gavrishchuk E.M., Kazantsev S.Yu., Kononov I.G., Rodin S.A., Firsov K.N. *Kvantovaya Elektron.*, **44** (6), 505 (2014) [*Quantum Electron.*, **44** (6), 505 (2014)].
12. Firsov K.N., Gavrishchuk E.M., Kazantsev S.Yu., Kononov I.G., Rodin S.A. *Laser Phys. Lett.*, **11** (8), 085001 (2014).
13. Firsov K.N., Gavrishchuk E.M., Kazantsev S.Yu., Kononov I.G., Maneshkin A.A., Mishchenko G.M., Nefedov S.M., Rodin S.A., Velikanov S.D., Yutkin I.M., Zaretsky N.A., Zotov E.A. *Laser Phys. Lett.*, **11**, 125004 (2014).
14. Velikanov S.D., Zaretskii N.A., Zotov E.A., Kozlovskii V.I., Korostelin Yu.V., Krokhin O.N., Maneshkin A.A., Podmar'kov Yu.P., Savinova S.A., Skasyrskii Ya.K., Frolov M.P., Chuvatkin R.S., Yutkin I.M. *Kvantovaya Elektron.*, **45** (1), 1 (2015) [*Quantum Electron.*, **45** (1), 1 (2015)].
15. Kozlovsky V.I., Akimov V.A., Frolov M.P., Korostelin Yu.V., Landman A.I., Martovitsky V.P., Mislavskii V.V., Podmar'kov Yu.P., Skasyrsky Ya.K., Voronov A.A. *Phys. Stat. Sol. B*, **247** (6), 1553 (2010).
16. Il'ichev N.N., Pashinin P.P., Gulyamova E.S., Bufetova G.A., Shapkin P.V., Nasibov A.S. *Kvantovaya Elektron.*, **44** (3), 213 (2014) [*Quantum Electron.*, **44** (3), 213 (2014)].

17. Apollonov V.V., Kazantsev S.Yu., Oreshkin V.F., Firsov K.N. *Kvantovaya Elektron*., **24** (3), 213 (1997) [*Quantum Electron*., **27** (3), 207 (1997)].
18. Velikanov S.D., Garanin S.G., Domazhirov A.P., Efanov E.M., Efanov M.V., Kazantsev S.Yu., Kodola B.E., Komarov Yu.N., Kononov I.G., Podlesnykh S.V., Sivachev A.A., Firsov K.N., Shchurov V.V., Yarin P.M. *Kvantovaya Elektron*., **40** (5), 393 (2010) [*Quantum Electron*., **40** (5), 393 (2010)].
19. Bulaev V.D., Gusev V.S., Kazantsev S.Yu., Kononov I.G., Lysenko S.L., Morozov Yu.B., Poznyshev A.N., Firsov K.N. *Kvantovaya Elektron*., **40** (7), 615 (2010) [*Quantum Electron*., **40** (7), 615 (2010)].
20. Velikanov S.D., Zapol'skii A.F., Frolov Yu.N. *Kvantovaya Elektron*., **24** (1), 11 (1997) [*Quantum Electron*., **27** (1), 9 (1997)].
21. Velikanov S.D., Evdokimov P.A., Zapol'skii A.F., Kovalev E.V., Pegoev I.N. *Kvantovaya Elektron*., **25** (10), 925 (1998) [*Quantum Electron*., **28** (10), 901 (1998)].
22. Rodin S.A., Balabanov S.S., Gavrishchuk E.M., Eremeikin O.N. *Opt. Zh*., **80** (5), 89 (2013).
23. Savin D.V., Gavrishchuk E.M., Ikonnikov V.B., Eremeikin O.N., Egorov A.S. *Kvantovaya Elektron*., **45** (1), 8 (2015) [*Quantum Electron*., **45** (1), 8 (2015)].
24. Balabanov S.S., Gavrishchuk E.M., Ikonnikov V.B., Rodin S.A., Savin D.V. Patent application PCT/RU2014/000605, dated 13.08.2014.
25. Timofeev O.V., Vilkova E.Yu. *Neor. Mater*., **46** (3), 297 (2010).
26. Devyatykh G.G., Gavrishchuk E.M., Korshunov I.A., et al. *Vysokochist. Veshchestva*, **2**, 34 (1993).
27. Andreev S.N., Firsov K.N., Kazantsev S.Yu., Kononov I.G., Samokhin A.A. *Laser Phys.*, **17** (6), 834 (2007).
28. Andreev S.N., Il'ichev N.N., Firsov K.N., Kazantsev S.Yu., Kononov I.G., Kulevskii L.A., Pashinin P.P. *Laser Phys.*, **17** (8), 1041 (2007).
29. Garnov S.V., Mikhailov V.A., Serov R.V., Smirnov V.A., Tsvetkov V.B., Shcherbakov I.A. *Kvantovaya Elektron*., **37** (10), 910 (2007) [*Quantum Electron*., **37** (10), 910 (2007)].